REPORT DOCUMENTATION PAGE

Form Approved
OMB No. 0704-0188

1. REPORT DATE *(DD-MM-YYYY)*	2. REPORT TYPE	3. DATES COVERED *(From - To)*
14-04-2007	Final	June 15, 2006 – January 14, 2007

4. TITLE AND SUBTITLE
Impact of Magneto-Electric Materials and Devices on Tactical Radio (and Radar)

5a. CONTRACT NUMBER
W911NF-06-C-0051

5b. GRANT NUMBER

5c. PROGRAM ELEMENT NUMBER

6. AUTHOR(S)
Dr. Jennifer Zinck, Dr. Christopher Henry, Dr. Deborah Kirby

5d. PROJECT NUMBER

5e. TASK NUMBER

5f. WORK UNIT NUMBER

7. PERFORMING ORGANIZATION NAME(S) AND ADDRESS(ES)
HRL Laboratories, LLC
3011 Malibu Canyon Road
Malibu, CA 90265

8. PERFORMING ORGANIZATION REPORT NUMBER

9. SPONSORING/MONITORING AGENCY NAME(S) AND ADDRESS(ES)
U.S. Army Research Office
P.O. Box 12211
Research Triangle Park, NC 27709-2211

10. SPONSOR/MONITOR'S ACRONYM(S)

11. SPONSORING/MONITORING AGENCY REPORT NUMBER
50975.1-MS-DRP

12. DISTRIBUTION AVAILABILITY STATEMENT
Approved for public release; distribution unlimited

13. SUPPLEMENTARY NOTES
The view, opinions and/or findings contained in this report are those of the author(s) and should not be construed as an official Department of the Army position, policy or decision, unless so designated by other documentation.

14. ABSTRACT
The interest in incorporating ME materials in electronic devices has been reinvigorated by the promising electric-field-based control of magnetization or magnetization-based control of polarization in monolithic materials. Primary screening of ME monolithic materials' based on their ferroelectric and magnetic ordering temperatures indicate they are not ready for application in devices and require further investment. Thus attention turned toward composite-based materials that magnetoelectrically couple through a strain field, which have known and beneficial properties, operate at room temperature or higher and can be modeled in a quasi-static fashion. While these composite materials may exhibit acceptable tunability and loss at low frequencies, strain nonuniformities, fabrication sensitivity, and proper evaluation of high frequency performance are still limitations. HFSS modeling to evaluate high frequency performance proved difficult because it cannot account for non-uniform magnetic fields nor magnetostrictive strain effects. Because of these current limitations, we recommend continued funding for ME materials' research and for development of modeling and engineering expertise to realize the potential of these novel materials.

15. SUBJECT TERMS
multiferroics, magnetoelectric materials

16. SECURITY CLASSIFICATION OF:			17. LIMITATION OF ABSTRACT	18. NUMBER OF PAGES	19a. NAME OF RESPONSIBLE PERSON
a. REPORT	b. ABSTRACT	c. THIS PAGE	UL	20	Christopher Henry
UNCLASSIFIED	UNCLASSIFIED	UNCLASSIFIED			19b. TELEPONE NUMBER (*Include area code*) 310-317-5174

HRL LABORATORIES

W911NF-06-C-0051

Impact of Magneto-Electric Materials and Devices on Tactical Radio (and Radar)

Dr. Jennifer Zinck, Dr. Christopher Henry and Dr. Deborah Kirby

HRL Laboratories, LLC
3011 Malibu Canyon Road
Malibu, CA 90265

April 2007

Final Report
Period Covered: June 15, 2006 – January 14, 2007

This material is based upon work supported by, or in part by, the U.S. Army Research Laboratory and the U.S. Army Research Office under contract number W911NF-06-C-0051.

U.S. Army Research Office
Attn: AMSRD-ARL-RO-OI (IPR)
P.O. Box 12211
Research Triangle Park, NC 27709-2211
IPR@aro.arl.army.mil

TABLE OF CONTENTS

LIST OF ILLUSTRATIONS

LIST OF TABLES

1. EXECUTIVE SUMMARY

Statement of the Problem Studied

This seedling study was meant to evaluate the potential of magneto-electric materials to impact size, weight and performance of tactical radio and radar systems. ME materials are a subclass of multifunctional materials that are distinguished by simultaneously having two or more of the following characteristics; ferromagnetism, ferroelectricity or ferroelasticity. As a consequence of this combined functionality such materials can exhibit:

- Wide dynamic frequency response as a consequence of spontaneous polarization and spontaneous magnetization
- Frequency dependent variable permeability and frequency dependent variable permittivity in a single device
- Magnetic properties controlled by electric field.

The goals of the seedling were to:

- Compile a database of material parameters specific to ME materials.
- Perform device simulations for a tunable filter architecture using materials parameters from the ME database for input.
- Benchmark tunable filter ME devices against state-of-the art devices presently in use for tactical radio and radar.
- Solicit expert input on risk/benefit analysis of tactical radio and radar systems based on ME devices.

Summary of Results

A database of properties for known single phase and composite ME materials was compiled which clearly showed that only composite ME materials were suitable at present for technological applications. A parametric study was performed using a heuristic model to show qualitatively the effect of various materials parameters on device tunability.

The benchmark ME device was a composite of a piezoelectric and magnetostrictive ferrite which displayed tunablilty of the ferromagnetic resonance by means of strain coupling (a second order ME effect). A significant impediment to achieving our goals of modeling this device was the discovery that existing commercial codes which claimed to treat ferrite materials could not accommodate the nonuniform magnetic fields associated with common device geometries and could also not incorporate magnetostriction in any meaningful way. Development of alternative code was beyond the scope of this seedling.

2. INTRODUCTION

Modern military tactical radio requires the ability to receive and transmit over an extremely large band of frequencies, from the low MHz well into the GHz range. This broadband environment differentiates military systems from the narrow bandwidth requirements of commercial technologies. The need for simultaneous regard over a very large bandwidth places very great demand on the linearity of the active and passive signal processing in military communication systems. Improvements in passive filter technology are expected to relax the demands on the active electronics in these systems, but at the expense of an impractical number of fixed frequency filters, or through the use of a more reasonable number of tunable filters. Varactor tuned filters can provide the required tuning range, but varactors are inherently non-linear due to the solid state physics behind the tuning mechanism. A key technology for flexible, low-power, and compact tactical radios is improved tuning elements for passive filters. Military radar has similar needs.

2.1 Issues Potentially Addressed by ME Materials and Devices

Like most applications, engineers of microwave and millimeter wave devices and subsystems trade cost, design and performance. When evaluating different technologies they look for:

- Component count vs. frequency,
- Tunability, cost vs. hysteretic loss,
- Cost vs. frequency tunability,
- Frequency tunability vs. hysteretic loss,
- Resistivity vs. quality factor,
- Degrees phase shift / db loss vs. tunability,
- Insertion loss.

Specifications that are important for nonreciprocal devices, such as circulators and isolators, are saturation magnetization, easy-axis or easy-plane anisotropy, anisotropy magnitude, magnetoelastic effects, dielectric constant, resistivity, power handling capability (limited by spin wave instabilities). These material properties can be engineered to meet the designer's performance criteria above for many RF applications. Yet increasing communications demands and needs have created a technological pull for materials and devices which require higher performance. Some of the "game changing" device characteristics brought up by the RF engineering community are:

- Circulators
    - Control impedance for improved uniformity;
- Phase shifters
    - True time delay
    - Independent control of phase and amplitude;
- Power dividers / combiners
    - Impedance transforming
    - Impedance maintenance;
- Low loss, high ε, wide band spiral radiators to protect LNAs.

The hope is that multiferroic and magnetoelectric materials and devices designed from them may help meet some of challenges RF engineers face. The results of this seedling show that the understanding of multiferroic materials, their capabilities / limitations and maturity level is warrants further investment.

3. TASK 1: DATABASE OF MAGNETO-ELECTRIC MATERIALS PROPERTIES

The benefits of incorporating magneto-electric (ME) materials in electronic devices has been reinvigorated by the promising developments of monolithic materials. Recently, intensive research has been conducted to optimize the magneto-electric effect in a number of different materials systems. Beyond the initial discovery of inherent magneto-electric effect in Cr_2O_3, other monolithic materials have been discovered that have exhibit a larger magneto-electric effect. Fiebig[1] gives a nice review of other ME materials that have been found and their ME effects: Ti_2O_3, ferrites such as ($GaFeO_3$, $BiFeO_3$ and YIG), boracites (such as $Ni_3B_7O_{13}I$), $BaMnF_4$, $TbPO_4$, mixed perovskites (such as $PbFe_{0.5}Nb_{0.5}O_3$), simple perovskites (such as $HoMnO_3$) and composites (such as PZT-Terfenol-D). Other possible candidate materials are thought to include colossal magnetoresistive oxides, pyrochlores, and other ferromagnetic oxides. Suitability of these materials for application has several criteria.

Primary screening of ME materials' readiness for application is determined by ferroelectric and magnetic ordering temperatures. Both Curie and Neél temperatures must be above the range of interest, in our case 200°C or greater. Secondarily, the ME coefficient must be a sufficiently large to be of technological interest. Thermodynamic limits of the linear ME tensor in monolithic materials are determined by electric, χ^e, and magnetic susceptibilities, χ^m, according to $\alpha_{ij}^2 < \chi_{ii}^e \chi_{jj}^m$, where α_{ij} is the induction of polarization by a magnetic field (direct effect) or magnetization by an electric field (converse effect). In composites, an effective ME effect occurs as a product property, which refers to novel effects stemming from the interaction between the composite constituent materials. Harshé et al.[2] developed expressions for an effective ME coefficient, α_{ij} for several conditions based upon the constituent materials properties of a magnetostrictive phase and piezoelectric or electrostrictive phase. These expressions have been revisited and refined in recent years by Nan *et al.*[3], Bichurin *et al.*[4], Srinivasan *et al.*[5]. The expression can be accomplished by combining magnetostrictive and piezoelectric materials for example:

$$ME\ effect = \frac{magnetic}{mechanical} \times \frac{mechanical}{electrical}.$$

Ideal ME material characteristics include low loss, phase stability over operating temperature, mechanical, magnetic and electrical ranges of interest, easily magnetized (μ_r

[1] Fiebig, J. Phys. D: Appl. Phys. **38** (2005) R123-R152
[2] G. Harshé, J.P. Dougherty and R.E. Newnham, Internatl. J. Appl. Electromagn. Matls., v4, p145-159, (1993)
[3] C.W. Nan, G. Liu, Y. Lin, PRL, 197203, 2005
[4] M.I. Bichurin, I.A. Kornev, V.M. Petrov, A.S. Tatarenko, Y.V. Killiba and G. Srinivasan, PRB, 64 094409, (2001)
[5] G. Srinivasan, M.I. Bichurin and V.M. Petrov, PRB 054402, 2003

> 100) and polarized (ε_r > 100) with low anisotropy and low coercivity, high saturation polarization (P_s > 20μC/cm^2), minimal defects for hysteretic scattering and oxygen diffusion and being amenable to a scalable manufacturing process. To date, most literature focuses on the direct ME effect, while of great interest for radio and radar is the converse effect, which has been illustrated at resonance by Shastry *et al* [6] and quasistatically by Ramesh[7]. Of importance, Ramesh reported coupling coefficient of 1×10^{-2} G cm/V. Enhanced properties can be achieved by exploiting epitaxial strains between thin films and device engineering for near resonance operation to maximize the ME effect.

The aim of this proposed program was to relate the unique characteristics of magneto-electric materials to device, and ultimately system performance. The specific application determines the needed characteristics of the device materials. Table 1 presents characteristics of candidate ME materials.

Table 1. Performance and Characteristics of ME Materials.

Material	Current characteristics	Reference
Single material	Temperature	
Cr_2O_3, Ti_2O_3	α_E = 4.1 ns/m	
Boracites: $M_3B_7O_{13}X$ *M* = Cr, Mn, Fe, Co, Cu, Ni. *X* = Cl, Br, I	$\varepsilon_r'\varepsilon_0\,\alpha_E$ =0.12 V/cm Oe, FE: T_C~100K AF or weak FM: High coercivity, saturation	Ascher *et al* 1966
Ba*M*F$_4$ / Li*M*PO$_4$ *M* = Mg, Mn, Fe, Co, Ni, Zn, Tb	α_E = 30-36 ns/m, FE: T_C~100K AF or weak FM: H = 20T, T_N ~25 K	Scott 1979 Rivera 1994, Kornev *et al* 2000
Perovskites: $AB'_{1-x}B''_xO_3$ A = Ba, Sr, Pb, B′= Fe, Co, Ni, B″ = Cr, Mo, W	Low transition temps, AF or weak FM High fields necessary	
Manganites: *R*MnO$_3$ *R* = Bi, Y, Nd, Tb, Dy, Ho, Er, In, Lu, Sc, Tm (CMR: PrCa, LaSr)	AF: T_N~70-130K, High H, FE: T_C~1000K Rich mag. behavior b/c frustrated system	Kimura LANL
Pyrochlores: A_2O-B_2O_6 A = BiZn, CaTi, BiFe, B = ZnNb, NbTi, FeNb	$\varepsilon_r'\varepsilon_0\,\alpha_E$ = 3 V/cm Oe, RT operation, high ε, Magnetic variant of microwave dielectrics	Vanderah NIST, Ubic et al.
Ferrites: *R*FeO$_3$ (YIG) *R* = Ba, Bi, Ni, Co, Zn, Mn,	α_E = 30 ns/m, Low resistivity, high fields	
Multi-material fabrication	Not scalable, strain coupling dependent, field nonuniformities	
Piezoelectric / Ferrite PZT, $BaTiO_3$ / Co, Ni, Li, NiZn Ferrites	Interdiffusion, bonding α_M acheived!	Srinivasan *et al* 2004 Ryu *et al* 2002
PZT-PVDF / Terfenol-D **PMN-PT / Terfenol-D**	$\varepsilon_r'\varepsilon_0\,\alpha_E$ = 4.68, 10.3 V/cm Oe, Low resistivity, bonding	Bichurin *et al* 2003 Ryu *et al 2002*

4. TASK 2: SIMULATIONS

4.1 Parametric Analysis of Impact of Strain on Tunability of FMR

Petrakovskii et al[8] have shown that the frequency shift of the ferromagnetic resonance for a spherical anisotropic ferromagnet subjected to a homogeneous uniaxial

[6] Shastry, G. Srinivasan, M. I. Bichurin, V. M. Petrov, and A. S. Tatarenko, Physical Review B 70, 064416 (2004)
[7] R. Ramesh, DARPA DSO Multiferroics Workshop, July 2005
[8] G. A. Petrakovskii and E. M. Smokotin, Soviet Physics JETP **28**, 1101 (1969)

compressive stress in the [110] axis and magnetized by a field H in the (110) plane is given by the relation;

$$\delta H(\theta,\sigma,k_1) = \frac{3\lambda_{100}\sigma}{2M_s} - \frac{9\sigma}{4M_s}(\lambda_{100}-\lambda_{111})\sin^2(\theta+\delta_{an})$$
$$+\frac{3\sigma}{2M_s}(\lambda_{100}-\lambda_{111})(1+\cos^2(\theta+\delta_{an}))-2\lambda_{100}) \quad (1)$$
$$\times\left\{\frac{4H_0}{H_a[\tfrac{9}{8}\sin^2 2(\theta+\delta)-\tfrac{3}{2}\sin^2(\theta+\delta)]}+\frac{H_a[\tfrac{9}{8}\sin^2 2(\theta+\delta)-\tfrac{3}{2}\sin^2(\theta+\delta)]}{2H_0}\right\}^{-1}$$

Where, $H_0 = \omega/|\gamma|$ is the applied magnetic field in Oersted, $H_a = 2K/M$ is the anisotropy field in Oersted, M = the saturation magnetization in Gauss, θ = the angle between the magnetizing field H and the [100] direction in radians, λ_{100}, λ_{111} = the magnetostrictive coefficients, K_1 = uniaxial anisotropy constant, σ = the applied stress in MPa, and δ = correction of the field direction due to presence of uniaxial anisotropy in radians (and/or elastic stresses[9]) given as:

$$\delta = -\frac{H_a \sin 2\theta\left[1-\tfrac{3}{2}\sin^2\theta\right]}{2H_0 + H_a\left[2-\sin^2\theta-3\sin^2 2\theta\right]}. \quad (2)$$

By inspection, one can see that the magnetic field shift is linear with stress and magnetostriction coefficients, while inversely proportional to saturation magnetization. The complex relationship of field angle and anisotropy, given by δ, gives the correction to theta due to the magnitude of the magnetocrystalline anisotropy as shown Figure 1 for three ferrites of technological interest, YIG, $CoFe_2O_4$ and BaM.

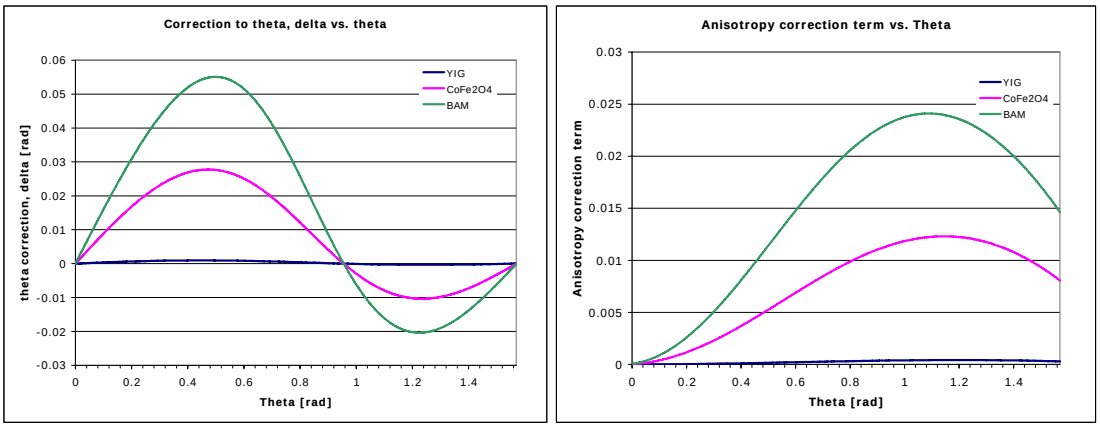

(a) **(b)**

Figure 1. (a) Theta correction due to anisotropy, (delta) vs. theta, (the cylindrical angle H_0 makes with the [100]-direction) for YIG $CoFe_2O_4$ and BaM. For most materials, this is a small correction on theta. (b) Anisotropy correction term (braces in Error! Reference source not found.**) vs. theta, the cylindrical angle H_0 makes with the [100]-direction for YIG $CoFe_2O_4$ and BaM. For most materials, this is a small correction to δH.**

[9] G. A. Petrakovskii and Yu. N. Kotyukov, Soviet Physics-Solid State, v7, n8, (1966).

Equation 1 has been used to model material tunability by varying applied stress and anisotropy-to-magnetostriction ratio. Values, in Table 2, for YIG and BaM are used because of technological importance and $CoFe_2O_4$ because of its large magnetostriction.

Table 2. Properties of Selected Ferrites used as input for Equation 1.

Property	YIG	$CoFe_2O_4$	BaM
M_s [G]	1750	4400	4420
H [Oe]	3400	12000	7500
K [erg/cc]	10^4	$2.6\ 10^6$	$3.2\ 10^6$
λ_{100}, λ_{111} [ppm]	-1.4, -1.6	-670, -120	-13, 0

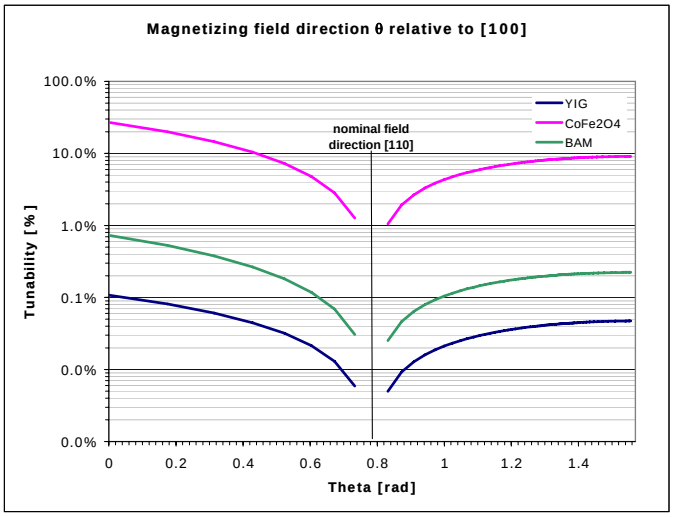

Figure 2. Ferrite tunability as a function of theta, the cylindrical angle H_0 makes with the [100]-direction, at stress -20 MPa. Thus, maximum tunability occurs when the field is aligned with the [100]-direction.

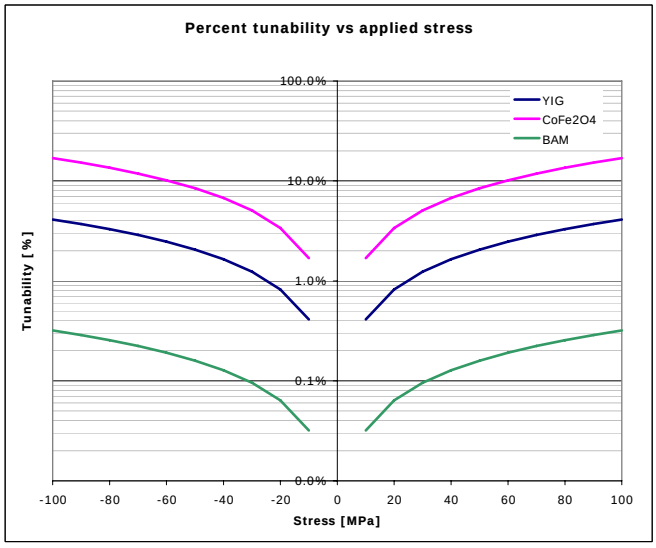

Figure 3. Ferrite tunability as a function of applied stress. Large magnetostriction from $CoFe_2O_4$ demonstrates the large effect that stress has on tunability. YIG has better tunability than BaM because of the much lower K_1 values.

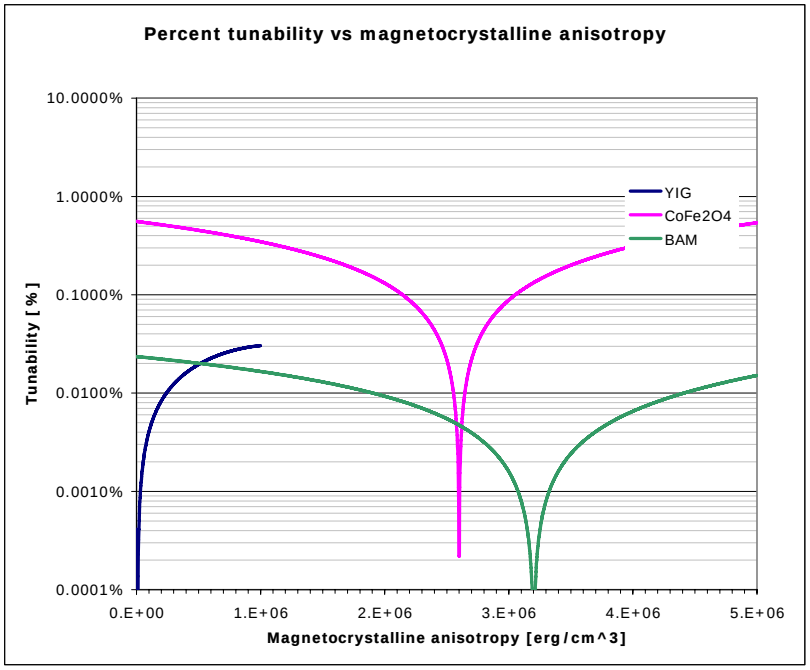

Figure 4. Ferrite tunability as a function of K_1. If K_1 were to change from its nominal value (Table 2), then tunability increases as anisotropy decreases.

4.2 Stress Induced FMR Tunability of Microwave Devices

Theoretical and experimental work that investigates tunability of FMR due to stress-induced effects is sparse. Dionne and Oates [10] use a mechanical fixture to apply compression into the plane of the Ni-Al spinel ferrite slab. They achieved tunability of 5% at 10.2 GHz due to high magnetostriction with a moderate magnetocrystalline anisotropy. For YIG under compression, they achieved ~50 MHz frequency shift at 2.9 GHz resulting in 1.7% tunability, which they attribute to the correspondingly lower magnetostriction-to-anisotropy ratio. For a piezoelectric-controlled ferrite device they believe:

> *"To reduce this concept to practice, the transmission of stress from piezoelectric to ferrite in a planar configuration needed to control a stripe domain pattern must be studied, to determine the most efficient and practical method. Because the ferrite must have a high magnetostriction-to-anisotropy ratio, the chemical composition of the ferrite must be tailored to optimize that property without degrading the permeability and propagation constants."*

In their patent [11], they suggest ferrites that have "strong inverse magnetostrictive properties sufficient to align magnetic domains and conventional piezoelectric materials which impart mechanical stress to the ferrite are the most promising to achieve a high magnetostriction-to-anisotropy ratio." These compositions follow:

[10] G.F. Dionne and D.E. Oates, Mater. Res. Soc. Symp. Proc. v833, (2005)
[11] G.F. Dionne and D.E. Oates, Tunable microwave magnetic devices, US patent 6,919,783, (2005)

- YIG garnet families
  - $Y_3Fe_{5-x-y}Al_xIn_yO_{12}$
  - $Y_3Fe_{5-x-y}Ga_xIn_yO_{12}$
  - $Y_3Fe_{5-x-y}Al_xSc_yO_{12}$
  - $Y_3Fe_{5-x-y}Ga_xSc_yO_{12}$
- Calcium-vanadium garnet families
  - $Y_{3-2x}Ca_{2x}Fe_{5-x-y}V_xIn_yO_{12}$
  - $Y_{3-2x}Ca_{2x}Fe_{5-x-y}V_xSc_yO_{12}$
  - $Y_{3-2x-y}Ca_{2x+y}Fe_{5-x-y}V_xZr_yO_{12}$
- Lithium, nickel, manganese, and magnesium spinel ferrite families
  - $Li_{0\ 5+t/2}Fe_{2.5-3t/2}Ti_tO_4$
  - $Li_{0.5-z/2}Zn_zFe_{2.5-z/2}O_4$
  - $Ni_{1-z}Zn_zFe_{2-x}Al_xO_4$
  - $Mn_{1-z}Zn_zFe_{2-x}Al_xO_4$
  - $Mg_1Fe_{2-x}Al_xO_4$

Srinivasan et al. [12] accomplished a resonance field shift of 40 Oe at E-fields of 8 kV/cm in a bilayer of 4.9μm (111) YIG and (001) PMN-PT with static E- and H-fields parallel to <111>. This is equivalent to 112 MHz shift, or 1.2% tunability at 9.3 GHz. The insertion losses from single-resonator filters can be theoretically estimated[13] to be -2.5 dB and have a tunability of 4.5% at 100 kV/cm, though practically it has been shown to be much greater than that, greater than -20 db.

Theoretical and experimental work that investigates ferromagnetic resonance and magneto-static waves under non-uniform conditions are few. Dikshteyn and Mal'tsev[14] bent a GGG substrate with a thin YIG film well below its elastic limit (0.02% strain, non-uniform stress of from 56 MPa at the root to average 28 MPa) and achieved 29 MHz frequency shift at a center frequency of 3.5 GHz, yielding a tunability of 0.8%. This is in close agreement with the results from **Error! Reference source not found.** in Figure 3.

4.3 HFSS Simulations of Tunable Filter

HFSS (High Frequency Structure Simulator) is a 3D full wave finite element field simulator code available from Ansoft Corporation. The current version of HFSS includes gyrotropic ferrite materials. However, during the course of this seedling it became clear that HFSS has two significant drawbacks which were not surmountable within the scope of this seedling. First, HFSS is only capable of simulating problems with homogeneous magnetic fields and is only strictly applicable to an ellipsoidal ferrite. Second, their appears to be no intuitive way to incorporate magnetostriction into the model using the available inputs to the code.

[12] G. Srinivasan, A.S. Tatarenko and M.I. Bichurin, Electronic Letters, v41, n10, (2005)
[13] P Carter, IEEE Trans. Microw. Theory Tech., v13, n3, (1965)
[14] I.Ye. Dikshteyn and O.A. Mal'tsev, J. of Comm. Tech. and Electronics, v38, n5, (1993)

4.4 Calculations of FMR as a Function of Internal Field

The prototype device was a PZT/YIG composite taken from the work of Tatarenko et al[15]. Measurements of insertion loss as a function of frequency for a saturation induction, $4\pi M$ of 1750 Gauss, FMR linewidth of 1 Oe, and an in plane applied field of 1700 Oe were shown to vary with electric field by over 100 MHz by the application of a 3kV/cm field across the PZT. A schematic of the device as input to HFSS is shown in Figure 5.

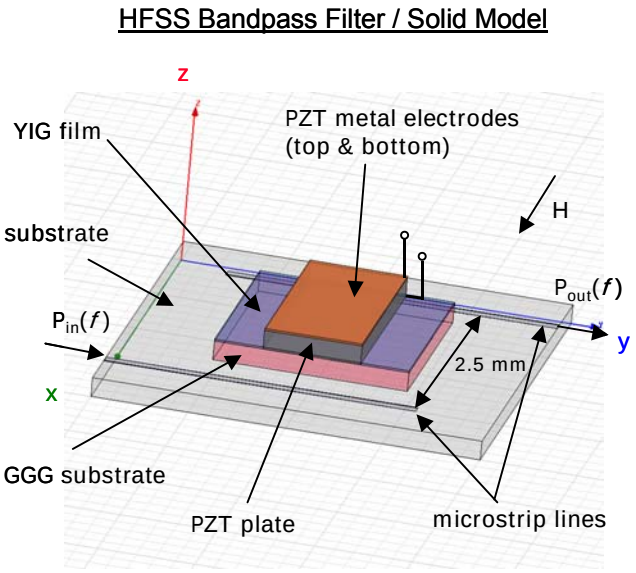

Figure 5. HFSS bandpass filter solid model from Tarantenko et al.

The device is simulated in HFSS as a symmetric 2-port device having a plane wave input to port 1 which excites an input microstrip line (18x1 mm). Radiation couples through the GGG substrate and into the YIG region (5mm × 1.5 mm × 110 μm). It couples under FMR back through the GGG substrate and out into the second microstrip line. Microstrip separation is 2.5 mm. Filter transmission (S21) is measured as the output at waveport 2 at the end of the second microstrip line.

Since we could not accommodate the magnetostriction directly, we solve static cases for varying magnitude internal H fields. In each case the internal H-field is uniform across the sample. It is assumed that this is closest equivalent possible to simulating the effect of the ferrite under magnetostriction at this time.

Materials properties used in the simulation are as follows. The lower substrate (alumina) under the microstrip lines has a dielectric constant of 10 and zero loss. To represent a lossy dielectric, a dielectric loss tangent, $\varepsilon''/\varepsilon'$ value for the material is applied. The greater the loss tangent, the more lossy the material. The GGG substrate has a dielectric constant of 7.7 and a dielectric loss tangent of 0.0002. The YIG element has a dielectric constant of 12 and a dielectric loss tangent of 0.0002, and a magnetic saturation value of 1750 Gauss. For the YIG, ΔH, the full resonance line width at half-maximum relates to how rapidly a precessional mode in the biased ferrite will damp out

[15] A. S. Tatarenko, V. Gheevarughese, and G. Srinivasen, Electronics Lett. **42**, xx (2006).

when the excitation is removed. In HFSS, the input parameter "delta H" varies with frequency and is therefore calculated within a simulation by

$$\text{delta } H = \Delta H * FREQ / F_{meas} \quad (3)$$

where ΔH corresponds to the measured linewidth at frequency F_{meas}, and FREQ is the HFSS swept frequency. In the simulations, ΔH = 3 Oe at 10 GHz.

The magnetic bias direction is set as per Tatarenko et al to be parallel to the sample and perpendicular to the microstrip lines and, in HFSS, it is set equal in magnitude to the magnetic saturation value (1750 Gauss). The port imepedance for this device is calculated to be approximately 40 ohms.

A simulation under these conditions, with H internal = 1000 Oe results in the transmission (S21), reflection (S11) and power loss (dB) as shown in Figure 8. The power lost is computed by the expression

$$P_{lost}\,(dB) = dB_{10}[1\text{-}mag(S11)^2\text{-}mag(S21)^2] \ . \quad (4)$$

Although in Figure 6 HFSS appears to reproduce the ferromagnetic resonance peak at 9.37 GHz expected for this system (with a loss of approximately –3dB), the linewidth is about a factor of 10 greater than expected. Since the linewidth is defined as 3 Oe at 10 GHz in the simulation parameters, we would expect to see a linewidth of this order in the result.

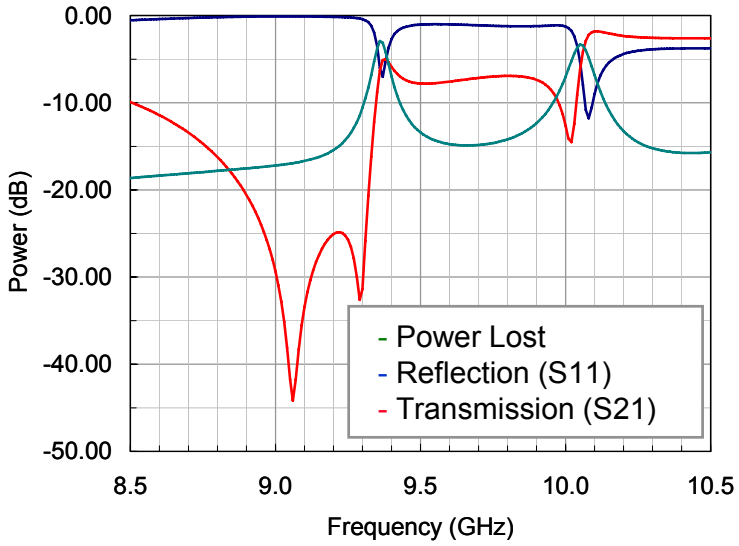

Figure 6. HFSS simulation result for the YIG filter device schematically represented in Figure 8. Active YIG sample (5x1.5 mm by 110 μm thick). FMR resonance is observed at 9.37 GHz. The loss is approximately –3 dB at 9.37 GHz. Hint = 1000 Oe. Magnetic saturation filed = 1750 Gauss.

In order to now attempt to model the effect of the magnetostriction, Figure 7 presents the simulation results of varying the internal field input to HFSS. While it looks like at an value of H_{int} = 2600 Oe there is 90 MHz of tuning over 100 Oe, it was unclear whether this represented tunability or a mode hopping. At low H_{int} fields, the FMR appears constant at around 9.3 GHz.

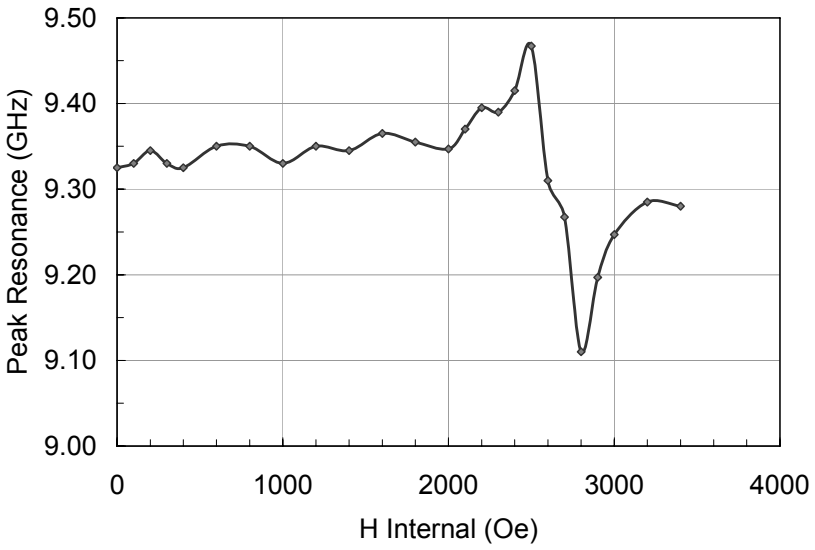

Figure 7. HFSS simulation result of FMR resonance frequency for varying internal magnetic field (H_{int}) for the YIG filter device schematically represented in Figure 6. Magnetic saturation field = 1750 Gauss. ΔH = 3 Oe at 10 GHz.

To investigate the effect of mode hopping, simulations were performed to observe the mode structure around the FMR resonance as H_{int} passes throughout this range. Simulations commenced at H_{int} = 2000 Oe which is below the observed resonance region of interest in Figure 7, and through H_{int} = 2900, at which point the negative shift in frequency was observed to be a maximum. Finally, we calculate at H_{int}=3200 Oe, where the FMR frequency appears to return towards its original value. Figures 8a) – e) present the results of these simulations. In Figure 8(a) and 8(b) one observes the primary FMR transmission resonance shift upward in frequency from 9.37 to 9.47 GHz with increased H_{int} as expected. Notice also in each case the presence of a quasi-static mode at about 10.1 GHz. In the next two Figures 8(c) and 8(d) we observe more mode mixing. As the internal field increases to 2600 Oe, the transmission resonance shifts to 9.57 GHz and weakens as additional modes appear at lower frequencies. For H_{int} increased to 2900 Oe, a small resonance remains at 9.81 GHz but a significant amount of mode mixing occurs, particularly around the quasi-static resonance. The 9.81 GHz mode becomes very weak and noisy as we observe a single stronger mode entering at lower frequency. At H_{int} = 3200 Oe the transmission spectrum returns to the values observed at lower H_{int} fields. It is again well defined and the FMR appears at 9.3 GHz. Figures 8(c) and 8(d) illustrate that there is significant modal structure for this device close to the FMR frequency for fields of H_{int} in the range 2600 – 2900 Oe, and that the potential for mode hopping clearly exists. It would be necessary to optimize the device design to reduce the number of modes present in the FMR tuning region in order to observe the effective tuning more clearly.

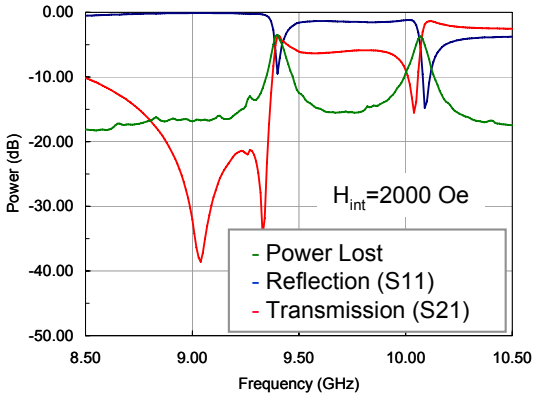

Figure 8(a). HFSS simulation result for the YIG filter device schematically represented in Figure 7. Active YIG sample (5××1.5 mm by 110 μm thick). FMR resonance is observed at 9.37 GHz. The loss is approximately –3.5dB at 9.37 GHz. Hint = 2000 Oe. Magnetic saturation field = 1750 Gauss.

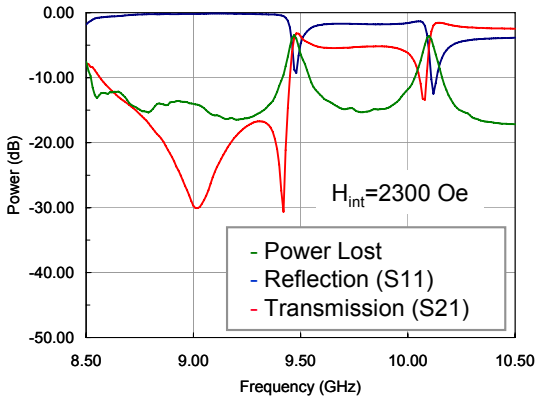

Figure 8(b). HFSS simulation result for the YIG filter device schematically represented in Figure 7. Active YIG sample (5×1.5 mm by 110 μm thick). FMR resonance is observed at 9.47 GHz. The loss is approximately –3.4dB at 9.47 GHz. Hint = 2300 Oe. Magnetic saturation field = 1750 Gauss.

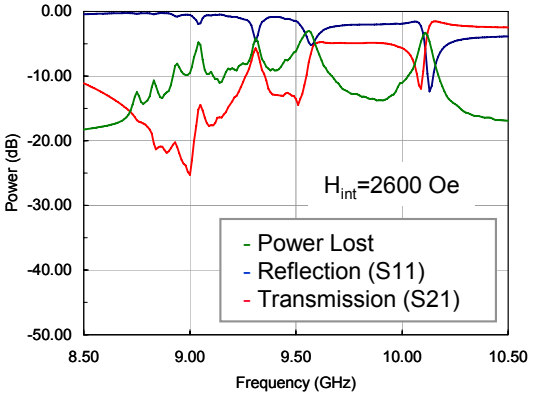

Figure 8(c). HFSS simulation result for the YIG filter device schematically represented in Figure 7. Active YIG sample (5x1.5 mm by 110 μm thick). FMR resonance is observed at 9.57 GHz. The loss is approximately –3.2dB at 9.57 GHz. Hint = 2600 Oe. Magnetic saturation field = 1750 Gauss. Note the second resonance at 10.11 GHz and –3.3 dB loss.

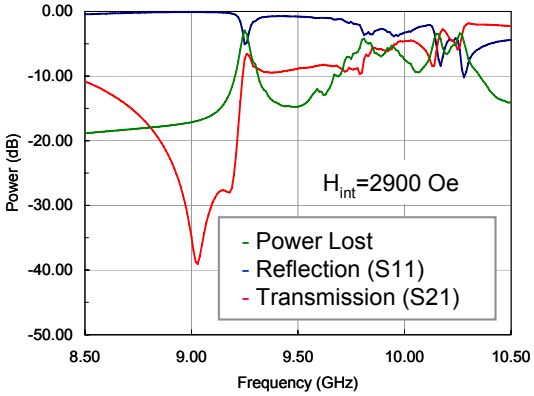

Figure 8(d). HFSS simulation result for the YIG filter device schematically represented in Figure 7. Active YIG sample (5x1.5 mm by 110 μm thick). FMR resonance is observed at 9.26 GHz. The loss is approximately –3.45dB at 9.26 GHz. Hint = 2900 Oe. Magnetic saturation field = 1750 Gauss. Note the second resonance at 10.16 GHz and –3.5 dB loss. Also, a weak resonance exists at 9.81 GHz with -4.2 dB loss.

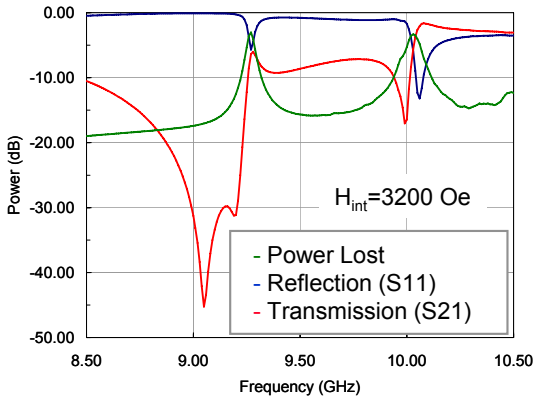

Figure 8(e). HFSS simulation result for the YIG filter device schematically represented in Figure 7. Active YIG sample (5x1.5 mm by 110 μm thick). FMR resonance is observed at 9.27 GHz. The loss is approximately –3.dB at 9.27 GHz. Hint = 3200 Oe. Magnetic saturation field = 1750 Gauss. Note the second resonance back at 10 GHz and –3.3 dB loss. The system has returned to its original state as in Figure 8a).

5. TASK 3: BENCHMARKING PROTOTYPE ME DEVICES AGAINST SOA

Data compiled in Table 3 represents the input solicited from engineers working in the areas of tactical radio and RADAR when queried about the figures of merit, present and future, for key system components.

Table 3. Specifications for Components used for Radio and Radar.

Device	***Current Materials***	***Desired Specs.***
Filters	Piezoelectric (SAW): very small; Metal/dielectric: (Stripline) simple and inexpensive Q_m =100-500; Quartz:: very high $Q_m = 10^4$	20% tunability around center freq; Q_m of 10,000 across bandwidth; ≤ -0.1 dB loss;
Isolators, circulators	Ferrites: handle large powers but bulky and requires large current	Isolation -100dB Control complex impedance <0.1dB across antenna dimension $10/pc
Phase shifters	GaAs: small and relatively inexpensive; Ferrites: handle large powers but bulky and requires large current	-0.1– -0.2 dB RMS loss across all phase and freq. settings Independent control of phase and amplitude 1ps – 10ns response time $10 / pc.

With reference to Table 3, and the assessment performed on this seedling we make the following conclusions:

1. Single phase materials still need significant investment to understand material physics and improve material properties.
2. Composite materials are ready for straight forward implementation. Sophisticated applications require additional modeling tools and materials advances.
3. Composite materials are better suited to low frequency applications. Millimeter wave applications have needs that are unmet and additional investment is needed to determine if multiferroic based composites can address those needs.
4. Multiferroics materials need to prove their superior performance in a field crowded with many technology alternatives.

6. TASK 4: RISK/BENEFIT ANALYSIS FOR ME DEVICES IN MILITARY SYSTEMS

It is difficult to make this analysis in general as every application has slightly different needs. Clearly, the field of ME materials and devices is immature. However, assuming that a strategic investment will result in successful maturation, the easiest benefits to visualize are in space-based applications where reduction in component size, weight or count represents a significant cost savings. For example, consider the non-linearity of a traveling wave tube power amplifier which is still the amplifier of choice for high power satellite communications. Complicated schemes have been devised to correct this nonlinearity in both hardware and software and have been successful for frequencies up to K band. However, as both military and commercial applications move to ever increasing bandwidth at higher transmit/receive frequencies new strategies must be developed. Table 4 gives the SWAP metric for the replacement of a predistortion phase equalizer with a ferrite/piezoelectric composite which is directly integrated into a waveguide. The integrated composite film-on-waveguide approach would potentially substantially improve the size and weight over currently used discrete components. Though the power requirement is marginally higher, the cost reduction for the reduced weight greater than x20.

Table 4. SWAP Metric for Film-on-Waveguide Equalization.

Solution vs. current	Film-on-waveguide		W-band (WR-10) waveguide	
SWAP metric	Individual device	Platform Total	Individual device	Platform Total
Size (in^3)	$2x10^{-5}$	0.005	0.044	10.5
Weight (lb)	0.0019	0.5	0.03	7.5
Power (W)	0.05	12	0	0
Device cost ($)	~50	~12K	~1K	240K
Launch cost ($)	19	5K	312	75K

7. SUMMARY

The interest in incorporating ME materials in electronic devices has been reinvigorated by the promising electric-field-based control of magnetization or magnetization-based control of polarization in monolithic materials. Primary screening of ME monolithic materials' based on their ferroelectric and magnetic ordering temperatures indicate they are not ready for application in devices and require further investment. Thus attention turned toward composite-based materials that magnetoelectrically couple through a strain field, which have known and beneficial properties, operate at room temperature or higher and can be modeled in a quasi-static fashion. While these composite materials may exhibit acceptable tunability and loss at low frequencies, strain nonuniformities, fabrication sensitivity, and proper evaluation of high frequency performance are still limitations. HFSS modeling to evaluate high frequency performance proved difficult because it cannot account for non-uniform magnetic fields nor magnetostrictive strain effects. Because of these current limitations, we recommend continued funding for ME materials' research and for development of modeling and engineering expertise to realize the potential of these novel materials.